

RESEARCH

Open Access



# MSCs with upregulated lipid metabolism block hematopoietic stem cell differentiation via exosomal CTP-1A in MDS

Chunlai Yin<sup>1†</sup>, Xue Yan<sup>1†</sup>, Jinyi Ren<sup>1</sup>, Cheng Zhang<sup>1</sup>, Jiaqing Liu<sup>1</sup>, Zilong Wang<sup>1</sup>, Jing Liu<sup>2</sup>, Weiping Li<sup>3\*</sup> and Xia Li<sup>1\*</sup>

## Abstract

**Background** Myelodysplastic syndrome (MDS) is a clonal disorder of hematopoietic stem cells (HSCs), characterized by ineffective hematopoiesis and a high risk of progression to acute myeloid leukemia. Elucidating the mechanism underlying the dysfunction of MDS-HSCs is crucial for exploring the pathogenesis of the syndrome. While previous studies have implicated mesenchymal stem cells (MSCs), a principal component of the bone marrow (BM) microenvironment, in the inhibition of normal hematopoiesis, the precise molecular mechanisms have not been fully elucidated. In this study, we investigated the effects of MSCs from MDS patients on hematopoietic functions of HSCs from a metabolic perspective.

**Methods** MSCs were isolated from BM of MDS patients. The proliferation, apoptosis, differentiation and support for hematopoiesis of these cells were analyzed using CCK-8 assay, FC and induction medium and CFU (colony forming units) assay, respectively. Expression levels of metabolic molecules were used as indicators to screen MSCs with different metabolic pathways and were detected by RT-PCR and Western blotting. Exosome derived from MSCs were isolated from the culture supernatant and confirmed by Transmission Electron Microscope, Dynamic Light Scattering and Western blotting. The effects of these exosomes on HSCs were analyzed using the same methods as those used to assess MSCs function.

**Results** Our findings demonstrated that MDS-MSCs exhibited significant functional impairments, including reduced proliferation, impaired differentiation, diminished support for hematopoiesis, and increased apoptosis. Notably, we observed an upregulation of lipid metabolism in these MSCs, which appears to contribute to their dysfunction. Intriguingly, the aberrant lipid metabolic profile can be effectively reversed by the administration of etomoxir (ETO), an inhibitor of carnitine palmitoyltransferase 1A (CPT-1A). Furthermore, MSCs with enhanced lipid metabolism could transmit this dysfunction to HSCs through the secretion of exosomes that are enriched in CPT-1A.

**Conclusions** We suggest that the MDS BM microenvironment disrupts MSCs metabolism by increasing the expression of CPT-1A, which impairs the ability to support normal HSCs. Interestingly, the suppressive effect is mediated

<sup>†</sup>Chunlai Yin and Xue Yan have contributed equally to this work and share first authorship.

\*Correspondence:

Weiping Li  
liweiping0910@sina.com  
Xia Li  
lixia416@163.com

Full list of author information is available at the end of the article



by exosomes rich in CPT-1A, which derived from MSCs. These findings provide novel insights into MDS MSCs-metabolism-Exosome axis in ineffective hematopoiesis and offer new strategies for the treatment of MDS.

**Keywords** Myelodysplastic syndrome, Mesenchymal stem cell, Hematopoietic stem cell, CPT-1A, Exosome

## Introduction

Myelodysplastic syndrome (MDS) arise from a small population of clonal disorder hematopoietic stem cells (HSCs) that characterized by aberrant differentiation, peripheral-blood cytopenia, and frequent progression to acute myeloid leukemia [1, 2]. Researchers have found that MDS show an increased incidence with age, often making it challenging to arrive at the appropriate diagnosis [3, 4]. Consequently, it is essential to explore the key mechanism in MDS so that retard the disease process or cure it for an aging society. In clinic practice, the therapy of this disease could be divided into two aspects. One is epigenetic therapy, which uses medicine such as azacitidine, decitabine to target the DNA hypermethylation to relieve symptom, but sometimes it is difficult to achieve a proper response for the patients [5]; Another is allogeneic HSCs transplantation, which treated as the only potentially curative option, but some studies indicate that the limited success of HSCs transplantation is attributed to the altered bone marrow (BM) microenvironment in MDS patients [6].

As one of the important components of BM microenvironment, mesenchymal stem cells (MSCs) can form a unique hematopoietic niche with HSCs [7–9], through secreting chemokine (C-X-C motif) CXCL12 to promote the homing of HSCs to the bone marrow [10], and releasing osteopontin to support HSCs expansion [11]. In addition, as multipotent cells, they can also differentiate into osteoblasts secreted chemokine CXCL12 ligand, stem cell factor (SCF), angiogenin, thrombopoietin [12], or into adipocytes secreted SCF to support HSCs hematopoietic function [13]. However, the regulatory role of MSCs on HSCs function in MDS is still controversial. Some researchers have found that MDS-MSCs exhibit functional changes, primarily characterized by reduced secretion of angiogenic factors, CXCL12, hematopoietic support cytokines, and proliferation compared to healthy controls [14–17]. Co-transplantation of BM-MSCs and HSCs has been shown to improve the success rate of transplantation in the MDS model [18]. However, some studies suggested that they haven't detected any quantitative or qualitative changes in MDS-MSCs [19]. These cells reportedly retain their typical morphology, growth characteristics, surface epitopes, differentiation potential, and immunophenotype [17, 20–22]. Therefore, the regulatory role of MDS-MSCs on HSCs requires further investigation.

Recent findings have indicated that metabolism plays an important role for the functions of MSCs including the differentiation potential [23, 24], migration, chemotactic localization [25], inflammatory response [26], tissue repair, and angiogenesis [27, 28]. However, the mechanisms by which MSCs metabolize and how these metabolic abnormalities affect the hematopoiesis of HSCs in the context of MDS require further investigation. In the present study, we investigated the mechanism by which dysfunctional MSCs impair normal hematopoiesis. MDS-MSCs suppressed normal hematopoiesis by shifting their metabolism towards lipid metabolism, which inhibited proliferation, differentiation, supporting for hematopoiesis and induced apoptosis in cells. Our integrated biological analyses demonstrated that exosomes secreted from MSCs play a crucial role in disrupting the function of HSCs, thereby suppressing the niche function that supports for normal hematopoiesis. Moreover, blocking CPT-1A with ETO to disrupt the lipid metabolism of MDS-MSCs restored the ability of these MSCs to support normal hematopoiesis. These data indicate that the impairment of metabolism, mediated by exosomes or their embedded CPT-1A, is a principal cause of BM failure in MDS and suggest that restoring the supportive niche could be a potential therapeutic approach.

## Methods

### Patient samples and controls

We included primary BM samples from diagnostic BM aspirations of  $n=21$  patients diagnosed with MDS. Patient characteristics are depicted in Table 1. As controls, primary BM from donors ( $n=10$  age ranges from 22 to 84 years) diagnosed with IDA (iron deficiency anemia) at the Department of Hematology, the Second Hospital of Dalian Medical University, China, was used. The use of primary material followed written informed consent of patients and approval by the ethics committee of the Second Hospital of Dalian Medical University (2019-151), in accordance with the Declaration of Helsinki. Samples were processed by Ficoll density gradient centrifugation to enrich for mononuclear cells (MNCs).

### Isolation and culture of bone marrow-derived MSCs

MSCs were isolated as described previously [29]. Briefly, Sterile bone marrow samples were centrifuged

**Table 1** Patients characteristics of the material used for in vitro experiments

NO	Disease	Age	Sex
1	IDA	60	M
2	IDA	72	M
3	IDA	63	M
4	IDA	36	F
5	IDA	84	F
6	IDA	67	M
7	IDA	49	F
8	IDA	22	F
9	IDA	69	F
10	IDA	56	F
11	MDS-EB2	47	F
12	MDS-EB1	56	M
13	MDS-EB1	65	M
14	MDS-EB2	73	M
15	MDS-EB1	77	M
16	MDS-MLD	52	F
17	MDS-MLD	34	M
18	MDS-EB1	67	F
19	MDS-MLD	89	M
20	MDS-EB1	60	F
21	MDS-MLD	67	F
22	MDS-EB1	73	F
23	MDS-EB1	74	M
24	MDS-EB1	71	M
25	MDS-EB2	61	M
26	MDS-EB1	59	M
27	MDS-EB2	82	M
28	MDS-RS	81	F
29	MDS-EB2	78	F
30	MDS-EB2	50	F
31	MDS-EB2	63	M

at 1500 rpm for 5 min, and the supernatant was collected and placed at  $-80^{\circ}\text{C}$ . An equal volume of  $1\times\text{PBS}$  solution was added to the supernatant, mixed thoroughly, and then added to 5 mL Ficoll, taking care to slowly add it to maintain a stable liquid level. After centrifugation at 800 g with slow acceleration and deceleration for 20 min, the MNCs were aspirated, washed with  $1\times\text{PBS}$ , seeded into T25 cell culture flasks and MSCs were enriched by their plastic adherence. The non-adherent cells were frozen after 24 h or culture with Human SCF (PeproTech), Human IL-6 (PeproTech), and Human IL-3 (PeproTech), while the remaining adherent cells were fed with half the volume of fresh medium every 3 days. Cells were stored viably in liquid nitrogen after 21 days.

### CCK-8 assay

MSCs from different groups were inoculated in 96-well cell culture plates with  $5\times 10^3$  per well. Cell proliferation was determined every 24 h by measuring absorbance at 450 nm with a Multiskan-FC (Thermo Fisher) according to the instructions of the CCK-8 kit (Vazyme).

### Apoptosis assay

The cells were treated according to the instructions of the eBioscience Annexin V-FITC Apop Kit (Thermo Fisher) and detected by flow cytometry. Finally, the data were statistically analyzed using Graphpad Prism software to plot the cell distribution. Three replicates were set for each group.

### Assay of adipogenic differentiation and osteogenic differentiation

MSCs were cultured with adipogenesis induction medium ( $\alpha$ -MEM containing 10% FBS, 5  $\mu\text{g}/\text{mL}$  insulin, 0.5 mmol/L 3-isobutyl-1-methylxanthine, and 1  $\mu\text{mol}/\text{L}$  dexamethasone) in 6-well plates with  $1\times 10^5$  cells per well for 14 days, and changed the culture medium every three days. Finally, Oil Red O staining was used to distinguish mature adipocytes from preadipocyte. For osteogenic differentiation, MSCs were inoculated in 6-well plates and cultured in freshly formed osteogenic medium (OM) for 21 days. Alizarin Red staining was used to detect bone mineralization.

### Colony forming unit (CFU) assay

Thawed MNCs ( $5\times 10^5$  cells per well) were cocultured with MSCs ( $1\times 10^4$  cells per well) in 48-well plates for 5 days. Then, MNCs ( $1\times 10^4$  cells per well) were cultured with methylcellulose media (MethoCult™ H4434 Classic, Stemcell) in 6-well plates for 14 days and colonies were counted using an inverted microscope.

### Real-time quantitative polymerase chain reaction

For quantification of gene expression, RNA was extracted from BM-MSCs of Control (They were diagnosed with IDA) or patients with MDS using a RNeasy Micro Kit or RNeasy Mini Kit (Qiagen). cDNA was synthesized from RNA using Superscript IV Reverse transcription (Thermo Fisher) ( $37^{\circ}\text{C}$  for 15 min,  $65^{\circ}\text{C}$  for 10 min). Real-time PCR analysis was set up with the SYBR Green qPCR Supermix kit (Invitrogen, Carlsbad, CA) and carried out in the iCycler thermal cycler. mRNA expression levels were calculated using the  $2^{-\Delta\Delta\text{Ct}}$  method with  $\beta$ -actin as the endogenous controls.

Name	Forward	Reverse
$\beta$ -actin	CATGTACGTTGCTAT CCAGGC	CTCCTTAATGTCACG CACGAT
SCF	ACCCAATGCGTGGAC TATCTG	GGCGACTCCGTTTAG CTGTT
IGF	CCTCTCAAGAGCCAC AAATGC	TCCAGCAGCCAAGAT TCAGA
CXCL12	TCAATTGCATCTCCC AGATAATGT	CACGTGCGTATAGGA ATTGG
LDHA	TTGACCTACGTGGCT TGAAG	GGTAACGGAATCGGG CTGAAT
G6PD	GGCCGTCACCAAGAA CATTG	TGGTCGATGCGGTAG ATCTG
CD36	CTTTGGCTTAATGAG ACTGGGAC	GCAACAACATCACC ACACCA
CPT-1A	TCCAGTTGGCTTATC GTGGTG	TCCAGAGTCCGATTG ATTTTTGC
CRAT	TTCACCGTGTGCCA GATGC	CAGCGTCTTGTCGAA CCAG
ACADVL	TCAGAGCATCGGTTT CAAAGG	AGGGCTCGGTTAGAC AGAAAG
HADHA	ATATGCCGCAATTTT ACAGGGT	ACCTGCAATAAAGCA GCCTGG

### Western blot analysis

MSCs or exosomes were lysed with RIPA peptide lysis buffer (Sevenbio, # SW104-02). Protein concentrations were determined by BCA method and separated on 10% sodium dodecyl sulfate polyacrylamide gel electrophoresis (SDS-PAGE). Then, the proteins were incubated with specific antibodies (1:1000). Anti-CD63 Rabbit pAb (Wanleibio, # WL02549), CPT1A (D3B3) Rabbit mAb (CST, #12252).

### Flow cytometry

Harvested cells were incubated with respective antibodies for 40 min at 4 °C after washing twice with 1×PBS. The antibodies utilized are listed in Table 2. All stained cells were measured using NovoCyte (Agilent). The data were analyzed with Novoexpress.

### Exosome isolation

Supernatants from MSCs with over 95% viability were collected, and exosomes were isolated by ultracentrifugation as described in MeilunBio (#MA0402). Briefly, cell culture medium was sequentially centrifuged at 300 g for 10 min, 2000 g for 30 min and 10,000 g for 70 min at 4 °C to remove dead cells and cell debris. Then, the supernatant was filtered through a 0.22  $\mu$ m filter, mixed with the extract agent, and incubated overnight at 4 °C. After incubation, centrifuged at 2~8 °C and 10,000 g for 1 h. The supernatant was aspirated and discarded, and the exosomes were found in the pellet at the bottom of the tube. The protein content of the concentrated exosomes

**Table 2** Antibodies of Flow cytometry used for in vitro experiments

Antibody	Company	Cat. No.
Anti-human CD90 PerCPCy5.5	eBioscience	45-0909-42
Anti-human CD105 PE	eBioscience	MHCD10504
Anti-human CD45 FITC	eBioscience	11-0459-42
Anti-human CD34 APC	Biolegend	343608
Anti-human Lineage (CD3/14/16/19/20/56) FITC	Biolegend	348801
Anti-human 7-AAD PerCPCy5.5	BD	559925

was measured using the BCA Protein Assay Kit (Sevenbio, # SW101-02). Each sample was diluted to a concentration of 2  $\mu$ g/ $\mu$ l with 1×PBS and stored at -80 °C for subsequent use.

### Electron microscopy

Exosomes were suspended in 1×PBS. 10  $\mu$ l of exosomes suspension were placed onto a copper grid and allowed to precipitate for 1 min, after which the excess liquid was blotted with filter paper. Then 10  $\mu$ l of acetate uranyl acetate was added to the copper grid and the grid was allowed to stand for an additional minute before blotting the excess liquid with filter paper. The grid was then left to air-dry at room temperature for several minutes. Electron microscopy imaging was performed at 100 kV using a Hitachi HT-7700 microscope. Transmission electron microscopy images were obtained.

### Nanoparticle tracking analysis

Nanoparticles were tracked using a Malvern Zetasizer Nano ZS90 (Malvern, UK) following the manufacturer's instructions. Exosomes derived from MSCs were diluted with 1×PBS (1:1000). The mean particle size and size distribution were analyzed by Dynamic Light Scattering (DLS) method through Malvern Zetasizer Nano ZS-90 (Malvern, UK).

### Statistical analysis

All data are presented as means  $\pm$  SD of three or more independent experiments. Statistical comparisons between two groups were performed using a Student's t-test. Oneway ANOVA followed by Tukey's post-hoc test was used to compare the differences among more than two groups, followed by the Bonferroni post hoc test. GraphPad Software Prism 6.0 was used for statistical analysis. Statistically significant differences were set at \* $p$  < 0.05, \*\* $p$  < 0.01.

## Results

### Evidence of BM-MSCs dysfunction in MDS

To analyze the function of MSCs, BM-derived cells were isolated from BM aspirates of patients diagnosed with MDS or Iron deficiency anemia (IDA) and were expanded *ex vivo* as previously described [29]. Primary MSCs were successfully obtained from all samples and showed a typical fibroblastoid elongated shape with the marker  $CD90^+CD105^+CD34^-CD45^-$  used for identification after 21 days (Figure S1A and S1B) [30, 31]. We found that the number of BM-MSCs in the MDS group significantly decreased during the process of *in vitro* culture, and this is in accordance with the findings of Giulia Corradi et al. [17]. To investigate the functional status of MDS-BM-MSCs, we assessed their proliferation ability using CCK8 and found that compared with the control group, the proliferation ability of MDS-MSCs was significantly reduced, with statistical significance at 24 h ( $p=0.0086$ ), 48 h ( $p=0.0441$ ), and 72 h ( $p=0.0093$ ) (Fig. 1A). Additionally, we observed an increase in the proportion of early apoptosis (Annexin  $V^+PI^-$ ) and late apoptosis (Annexin  $V^+PI^+$ ) cells in MDS-MSCs compared with the control group (Fig. 1B). BM-MSCs can differentiate into various bone marrow stromal cells, including osteoblasts and adipocytes, which are essential components of the bone marrow niche [32]. We observed significant Oil Red O (left) or Alizarin red (right) positive staining in osteogenic-differentiated and adipogenic-differentiated MSCs cultures, respectively. Interestingly, there were significant differences detected in the intensity of differentiation-specific staining in MDS-MSCs compared with IDA-MSCs, suggesting a reduced differentiation capacity of MSCs precursors in MDS patients (Fig. 1C, D). Furthermore, we detected the expression of related hematopoietic factors in MDS-MSCs and found that the expression of SCF was significantly down-regulated compared with the control group, while IGF and CXCL12 showed a downward trend. (Fig. 1E). To investigate the effect of MSCs on HSCs differentiation, we co-cultured MDS-MSCs with IDA-BM-MNCs *in vitro* and found a significant reduction in the apoptosis of  $CD34^+$  cells in IDA-BM-MNCs from MDS group (Fig. 1F). Additionally, the percentage of  $CD90^+$  cells was significantly lower in the Lineage- $CD34^+$  cells after co-culture, indicating that MDS-MSCs may impair the population of long-term HSCs in the BM (Fig. 1G and S2). To confirm the effect of MDS-MSCs on HSCs differentiation, we assessed colony formation of MNCs through methylcellulose Colony forming unit (CFU) assay. The results revealed impaired colony formation in the MDS-MSC samples compared to those from

IDA patients, characterized by the smaller size of CFU, which was consistent with their defective apoptosis and the presence of aberrant cell subsets (Fig. 1H).

### Metabolism of MDS-MSCs shifted towards lipid metabolism

We analyzed the glycometabolism in MDS-MSCs using RT-PCR to detect the essential enzyme and found it decreased significantly (data not shown). We believed that there was an energy metabolism shifted in MDS-MSCs when glycolysis was downregulated. Next, we analyzed the expression of genes related to lipid metabolism. The results showed that compared with the control group, the expression of CD36, a molecule involved in fatty acid transport, was significantly upregulated in MDS-MSCs. Meanwhile, the expression of CPT-1A, a key enzyme in fatty acid oxidation, was also significantly increased. Although there were no significant differences in the expression of CRAT, ACADVL, and HADHA, which are related to fatty acid oxidation, their expression showed an upward trend (Fig. 2A). Protein level showed the same phenomenon that the expression of CPT-1A in MDS-MSCs was significantly upregulated compared to the control group (Fig. 2B). We speculated that when glycolysis is abnormal in MDS-MSCs, the cell's energy supply shifted towards lipid metabolism to keep energy balance.

To explore the impact of lipid metabolism deviation on MDS-MSCs function, we used ETO (Sigma) to inhibit the function of CPT-1A and investigated MSCs function again. The results showed that the proliferation capacity of MDS-MSCs significantly increased following ETO treatment, compared with the untreated control group (Fig. 3A). Additionally, this treatment decreased the apoptosis of MDS-MSCs, especially early apoptosis ( $p=0.0048$ ) (Fig. 3B), and restored the adipogenic and osteogenic abilities (Fig. 3C, D). To explore the impact of treated MDS-MSCs on HSCs, we co-cultured MDS-MSCs with IDA-MNCs before or after blocking CPT-1A. The results showed that compared with the untreated group, the apoptosis of  $CD34^+$  IDA-MNCs increased after co-culturing with MDS-MSCs pretreated with ETO (Fig. 3E). Additionally, the proportion of  $CD90^+$  cells in Lineage- $CD34^+$  IDA-MNCs significantly increased ( $p=0.013$ ) (Fig. 3F). At the same time, the colony formation ability of IDA-MNCs co-cultured with ETO-pretreated MDS-MSCs significantly recovered (Fig. 3G), indicating that the function of MDS-MSCs partially recovered.

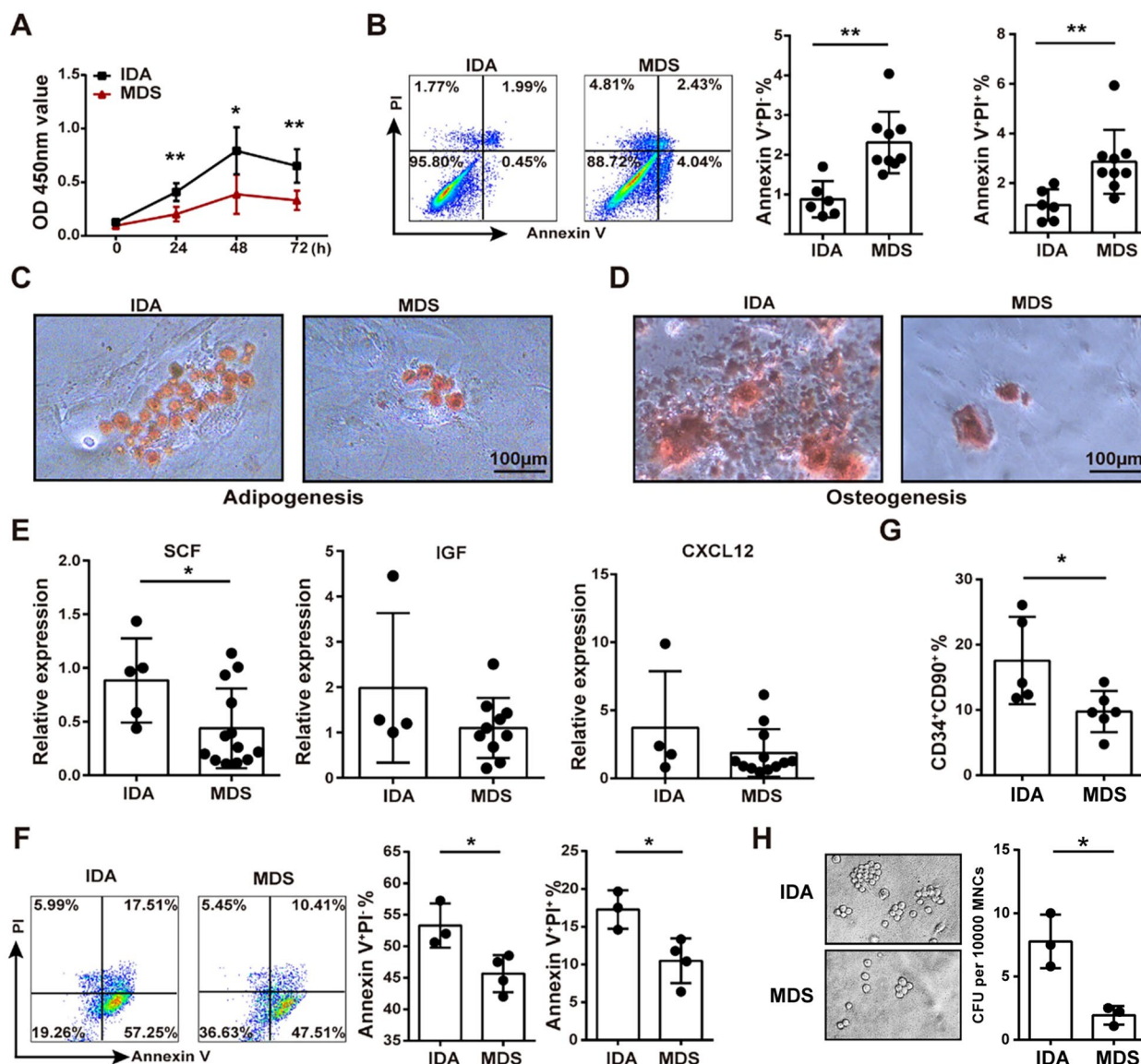


**Fig. 1** Evidence of BM-MSCs dysfunction in MDS. **A** The proliferation of BM-MSCs analyzed with the CCK8 assay. **B** The apoptosis of BM-MSCs analyzed with Flow cytometry. **C** Oil Red O staining analyzed adipogenic differentiation of BM-MSCs. **D** Alizarin Red staining analyzed osteogenic differentiation of BM-MSCs. **E** The expression of hematopoiesis-related genes in MSCs were analyzed by RT-PCR. **F** The apoptosis of CD34<sup>+</sup> MNCs that co-cultured with BM-MSCs for 24 h analyzed with Flow cytometry. **G** The percentage of CD90<sup>+</sup> cells in the Lineage-CD34<sup>+</sup> cells that co-cultured with BM-MSCs for 24 h analyzed with Flow cytometry. **H** CFU-colony forming of MNCs were analyzed after co-incubation with MSCs. (\*\*\*)*p* < 0.001, \*\**p* < 0.01 and \**p* < 0.05 compared with control)

### Exosomes from MDS-MSCs inherit the lipid metabolism abnormalities blocking the hematopoietic differentiation of HSCs

To further explore the mechanism by which MDS-MSCs with lipid metabolism abnormalities regulate HSCs and exacerbate the progression of MDS, we analyzed the GEO database (GSE140101) of MDS-MSCs and found that compared with healthy controls (HC), the expression of vesicle transport-related genes was upregulated

in MDS-MSCs (Fig. 4A, B). Additionally, differentially expressed genes were enriched in physiological processes related to membrane composition changes (Fig. 4C).

Exosome, one products of vesicle transport under lipid metabolism regulation, can mediate exchange of cell membrane constituents and regulate the target cells' function [33]. To investigate whether exosomes secreted by MSCs affect the hematopoietic function of HSCs, we first isolated exosomes from the culture supernatant of

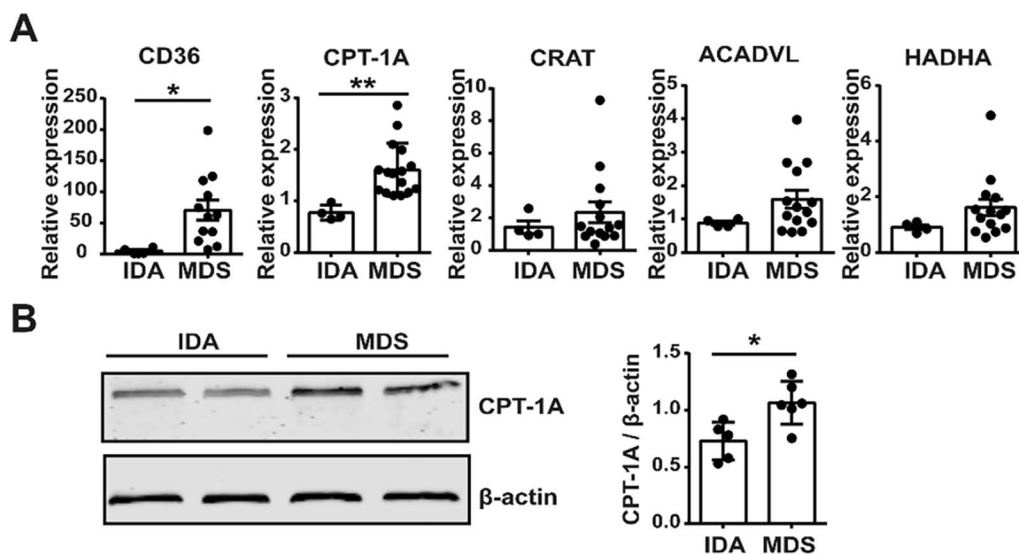


**Fig. 2** The up-regulation of lipid metabolism in MDS-MSCs. **A** The expression of genes related to lipid metabolism in MSCs were analyzed by RT-PCR. **B** The level of CPT-1A were detected by Western Blotting. Full-length blots/gels are presented in Supplementary Western Blot files. (\*\* $p < 0.01$ , \*\* $p < 0.01$  and \* $p < 0.05$  compared with control)

BM-MSCs using exosome extraction kit. Subsequently, exosomes were verified as small vesicles of approximately 100 nm in size by transmission electron microscopy (TEM), and their expression of CD63 was confirmed (Fig. 4D). The size distribution of the exosomes was predominantly within the range of 50–150 nm (Fig. 4E). Interestingly, protein content analysis showed a significant increase in exosome content in the culture supernatant of MDS-MSCs (Fig. 4F), indicating that vesicle transport pathways may play a regulatory role by enhancing exosome secretion. To explore whether exosomes from MDS-MSCs inherit the function of blocking HSCs hematopoiesis, we co-incubated exosomes from MDS-MSCs with IDA-MNCs in vitro. The results indicated that after treatment, the colony formation of the cells was significantly reduced compared to the exosomes untreated group (Fig. 4G). Although there was no significant difference in the positive expression rate of CD90 in Lineage<sup>-</sup>CD34<sup>+</sup>IDA-BM-MNCs, there was a downward trend (Fig. 4H). Additionally, analysis after exosome incubation also found that compared with the control group, the cells apoptosis was significantly reduced in MDS-MSCs' exosomes treated group (Fig. 4I). This is consistent with the previous results of decreased HSCs apoptosis after MDS-MSCs treatment.

To verify that exosomes from MDS-MSCs inherit the lipid metabolism abnormalities and impaired HSCs hematopoiesis through their contents, we first determined the protein molecular weight range of exosome contents using protein gel staining. The results revealed protein expression around 170 kD, 80 kD, and 50 kD

(Fig. S3A). Subsequently, we detected the content of lipid metabolism-related enzymes in the above molecular weight range of exosomes by Western Blotting. The results showed that compared with IDA-MSCs, the content of CPT-1A in exosomes from MDS-MSCs significantly increased (Fig. 4). This suggested that exosomes may regulate HSCs hematopoiesis by carrying abundant CPT-1A, which is inherited from MDS-MSCs with abnormal lipid metabolism. Since the production of exosomes is closely related to the lipid metabolism, which is inhibited by ETO, we investigated the changes in the content of exosomes in cell culture supernatant after treating the cells with ETO for 48 h. However, there was no significant change in the content of exosomes in the culture supernatant of MDS-MSCs after treatment (Fig. S3B).

Does the supportive effect of MDS-MSCs exosomes on HSCs hematopoiesis recover after ETO treatment? We extracted exosomes from the culture supernatant of MDS-MSCs after ETO pre-treatment, and co-incubated them with IDA-MNCs. Compared with the control group, exosomes derived from MDS-MSCs after ETO treatment significantly increased apoptosis in CD34<sup>+</sup> IDA-MNC cells (Fig. 5A). Moreover, although there was no significant difference in the positive rate of CD90<sup>+</sup> cells in Lineage<sup>-</sup>CD34<sup>+</sup> IDA-MNC cells (Fig. 5B), the colony-forming ability of IDA-MNCs co-incubated with conditioned exosome significantly recovered (Fig. 5C). This suggests that after ETO treatment, exosomes from MDS-MSCs regain their supportive roles for HSCs hematopoiesis.

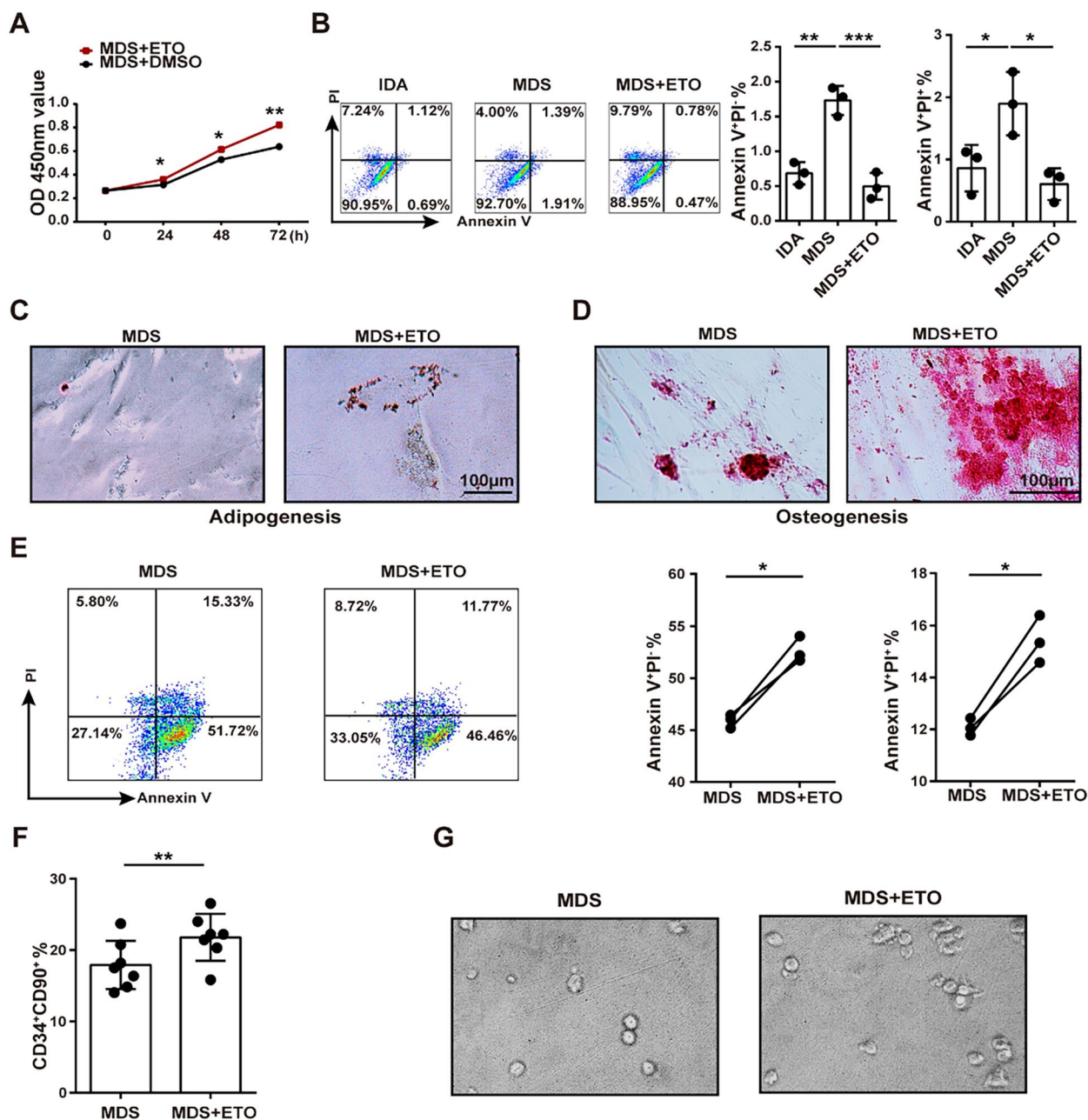


**Fig. 3** Blocking CPT-1A by ETO can restore the function of MDS-MSCs. **A** The proliferation of BM-MSCs pre-treated for 24 h by ETO analyzed with the CCK8 assay. **B** The apoptosis of BM-MSCs pre-treated for 24 h analyzed with Flow cytometry. **C** Oil Red O staining analyzed adipogenic differentiation of BM-MSCs with 100 µmol/L DMSO or ETO. **D** Alizarin Red staining analyzed osteogenic differentiation of BM-MSCs with 100 µmol/L DMSO or ETO. **E** The apoptosis of CD34<sup>+</sup> MNCs that co-cultured with BM-MSCs that per-treated with ETO for 24 h analyzed with Flow cytometry. **F** The percentage of CD90<sup>+</sup> cells in the Lineage-CD34<sup>+</sup> cells that co-cultured with BM-MSCs that per-treated with ETO for 24 h analyzed with Flow cytometry. **G** CFU-colony forming of MNCs were analyzed after co-incubation with MSCs. (\*\**p* < 0.001, \*\**p* < 0.01 and \**p* < 0.05 compared with control)

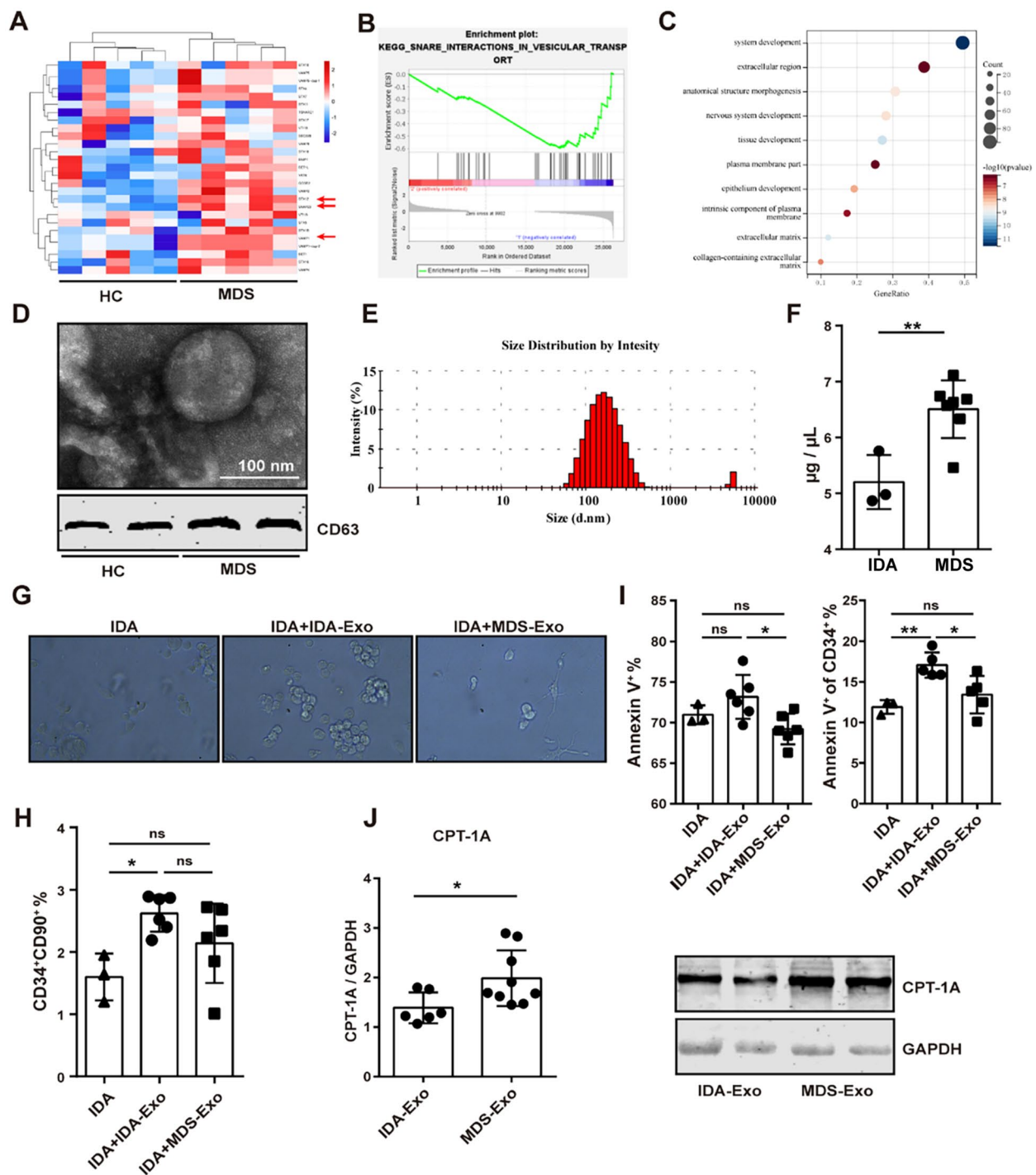


**Fig. 4** Exosome derived from MDS-MSCs enriched with CPT-1A and impeded the hematopoietic differentiation of HSCs. **A** Heatmap of the dysregulated RNA expression profiles in HD and MDS patients in GSE140101. **B** and **C** Functional enrichment analysis up-regulation in MSCs from MDS patients through KEGG pathway and GO terms. **D** Transmission electron microscopy (TEM) of exosomes isolated from the supernatant of MSCs and the expression of exosome-specific markers CD63 analyzed by western blotting. **E** Size distribution and concentration of exosomes were measured by Nanoparticle Tracking Analysis. **F** The content of exosomes from the supernatant of MSCs were measured by BCA kit. **G** CFU-colony forming of MNCs treated with 50  $\mu\text{g}/\text{mL}$  exosomes were analyzed. **H** The percentage of CD90<sup>+</sup> cells in the Lineage-CD34<sup>+</sup> cells that co-cultured with 50  $\mu\text{g}/\text{mL}$  exosomes for 24 h analyzed with Flow cytometry. **I** The apoptosis of MNCs (left) and CD34<sup>+</sup> MNCs (right) that co-cultured with 50  $\mu\text{g}/\text{mL}$  exosomes for 24 h analyzed with Flow cytometry. **J** The level of CPT-1A in exosomes were detected by Western Blotting. Full-length blots/gels are presented in Supplementary Western Blot files. (\*\* $p < 0.001$ , \*\* $p < 0.01$  and \* $p < 0.05$  compared with control)

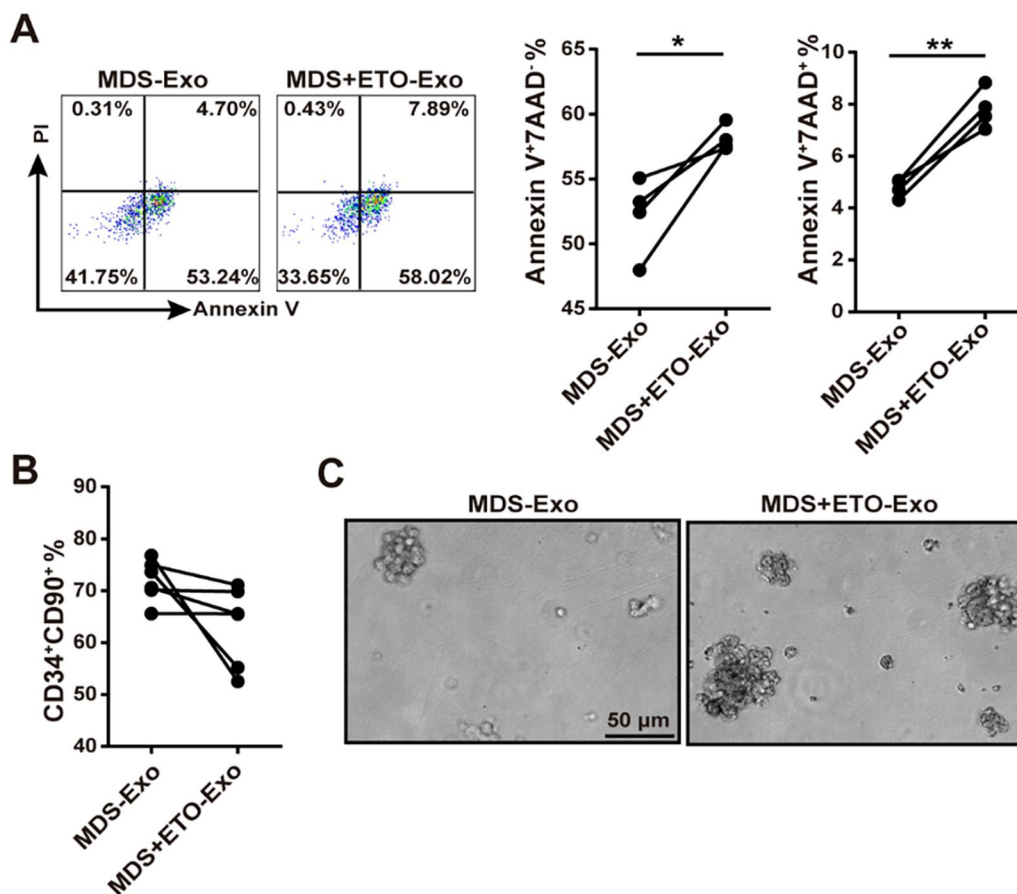


**Fig. 5** After blocking CPT-1A, the function of MDS-BM-MSc exosomes in supporting HSC hematopoietic differentiation can be restored. **A** The apoptosis of CD34<sup>+</sup> MNCs (right) that co-cultured with 50 μg/mL exosomes derived from MSCs with or without ETO for 24 h analyzed with Flow cytometry. **B** The percentage of CD90<sup>+</sup> cells in the Lineage-CD34<sup>+</sup> cells that co-cultured with 50 μg/mL exosomes derived from MSCs with or without ETO for 24 h analyzed with Flow cytometry. **C** CFU-colony forming of MNCs treated with 50 μg/mL exosomes derived from MSCs with or without ETO were analyzed. (\*\*\*)*p* < 0.001, (\*\*)*p* < 0.01 and (\**p* < 0.05 compared with control)

### Discussion

Myelodysplastic syndrome (MDS) is commonly considered a pre-malignancy in the elderly [34], and its progression is closely related to MSCs in the bone marrow microenvironment [35]. However, the precise mechanism remains unclear, severely limiting the application of MSCs in the diagnosis and treatment of MDS. Our results revealed that MDS-MSCs exhibited reduced proliferation, elevated apoptosis, diminished osteogenic and adipogenic potential, and altered cell metabolism; these alterations collectively contribute to the suppression of hematopoietic function in HSCs. Further analysis revealed a shift in energy metabolism towards lipid metabolism, characterized by the upregulation of lipid metabolism-related gene CPT-1A, which directly regulated the functions of MDS-MSCs. Additionally, the vesicular transport pathway, closely linked to lipid metabolism, influenced HSCs hematopoietic function through exosomes enriched with CPT-1A. In summary,

our study suggests that the dysregulated upregulation of lipid metabolism in MDS-MSCs could impair their hematopoietic supportive capacity by secreting exosome enriched in CPT-1A.

While some studies have observed weakened expansion capacity of MDS-MSCs compared to healthy controls [36, 37], others suggest similar proliferation rates between MDS-MSCs and healthy controls [38, 39]. These differences in MSCs functional status may be attributed to varying disease severities among patients and differences in in vitro culture systems. In our study, all samples were obtained from high-risk MDS patients. After successfully isolating MSCs from the bone marrow of MDS patients, we confirmed a significantly reduction in cell proliferation, along with increased cell apoptosis. The slow growth and decreased cell number of MSCs may contribute to their reduced support of hematopoiesis. Additionally, osteoblasts and adipocytes are crucial sources of cytokines such as stem cell

growth factors that maintain the function of hematopoietic stem cells [40]. However, controversy exists regarding the alterations in osteogenic and adipogenic potential of MDS-MSCs. Whereas some researchers report diminished the osteogenic and adipogenic capacities [41], others have found no significant changes in differentiation potential [17]. Our findings indicated that the osteogenic and adipogenic differentiation abilities of MDS-MSCs were indeed weakened, potentially leading to the loss of hematopoietic niche and supportive factors for hematopoiesis, thereby impairing HSCs hematopoietic function. Nevertheless, constrained by the paucity of bone marrow samples from healthy controls, we elected to employ cells from individuals with iron deficiency anemia (IDA) a comparison group. This choice was based not only on the clinical similarities between IDA and MDS, but also on the understanding that IDA is primarily due to nutritional deficiencies that influence erythropoiesis, rather than causing direct damage to the HSCs. This phenomenon requires further confirmation in healthy controls and mouse model.

Studies have revealed that CD34<sup>+</sup>CD90<sup>+</sup> HSCs, characterized as long-term HSCs accumulated in MDS patients [1], play a pivotal role in BM regeneration and multilineage hematopoiesis [42, 43]. Therefore, when assessed the hematopoietic potential of HSCs, we detected the percentage of CD90<sup>+</sup> cells within the Lineage<sup>-</sup>CD34<sup>+</sup> cell population of IDA BM mononuclear cells (IDA-BM-MNCs) after co-incubating with MDS-MSCs for 24 h. The reduction in the subpopulation of hematopoietic cells supports our viewpoint that MDS-MSCs inhibited HSCs hematopoiesis. However, CD34<sup>+</sup>CD90<sup>+</sup> cells are not the sole cell population contributing to the abnormal hematopoietic process, such the common myeloid progenitors and granulocyte-monocyte progenitors also accumulated in MDS [1]. To further validate our findings, we assessed the colony-forming ability of IDA-BM-MNCs, rather than HSCs due to the limited number of cells, using experimental methods commonly employed in the functional evaluation of MDS-HSCs [44]. We arrived at the same conclusion, reinforcing the inhibitory effect of MDS-MSCs on hematopoiesis. It has been reported that the dysfunction of HSCs at the early stage of MDS BM may be attributed to aberrant apoptosis [45, 46], whereas advanced MDS progressing to AML is characterized by the accumulation of immature cells in the BM with a decrease in cell apoptosis [47, 48]. Our research demonstrated a significant decreased in cell apoptosis of CD34<sup>+</sup>Lineage<sup>-</sup> IDA-MNCs

after co-culturing with MDS-MSCs, highlighting the distinct characteristics exhibited at different disease stages. This suggested to us that precise analysis tailored to individual patients is imperative to understanding these variations.

The function of BM-MSCs is intricately linked to metabolism [49, 50], which reports suggest that enhancing glycolysis can boost their immune functions and therapeutic potential, while inflammatory stimulation primarily alters their lipid metabolism [51]. We initially assessed the metabolic state by examining the expression of genes related to glycolipid metabolism to evaluate aerobic oxidation, glycolysis, and the pentose phosphate pathway (data not shown). Preliminary results indicated a downregulation of glycolysis in MDS-MSCs, although we were unable to pinpoint which cellular functions are primarily affected by these changes. Interestingly, when investigated the expression of genes related with lipid metabolism, we observed a significant upregulation, suggesting a metabolic imbalance in the cells. Studies have shown that AML-MSCs exhibit altered lipid metabolism, with a decrease in lipid content during the differentiation and a propensity towards adipocyte differentiation, thereby promoting the formation of the HSCs niche under pathological conditions [52]. Our findings indicated that the abnormal upregulation of lipid metabolism in MDS-MSCs may be linked to lipid breakdown during MSCs differentiation, resulting in a decreased lipid level. Furthermore, after inhibiting the function of CPT-1A, a key enzyme in fatty acid oxidation, the hematopoiesis-promoting function of MDS-MSCs was enhanced, suggesting a pivotal role of lipid metabolism in the functional regulation of MDS-MSCs. Although we collected a total of 21 clinical samples for all the experiments, the inherent heterogeneity among the patient samples made it challenging to identify distinct differences in MSC metabolism across various subtypes with such a limited sample size. Consequently, we did not categorize them into separate subtypes for comparative analysis.

Lipid metabolism emerged as a crucial factor governing cell proliferation, notably showing a significant decrease in MDS-MSCs in our study. We were intrigued by how lipid metabolism regulated the function of HSCs. Bioinformatics analysis uncovered notable changes in the vesicular transport pathway, regulated by lipid metabolism. Studies on exosomes, which are related to vesicular transport pathway and characterized by a size of 30–150 nm and contain various functional molecules, have highlighted their role in transferring information between cells and altering target cells phenotype. Also,

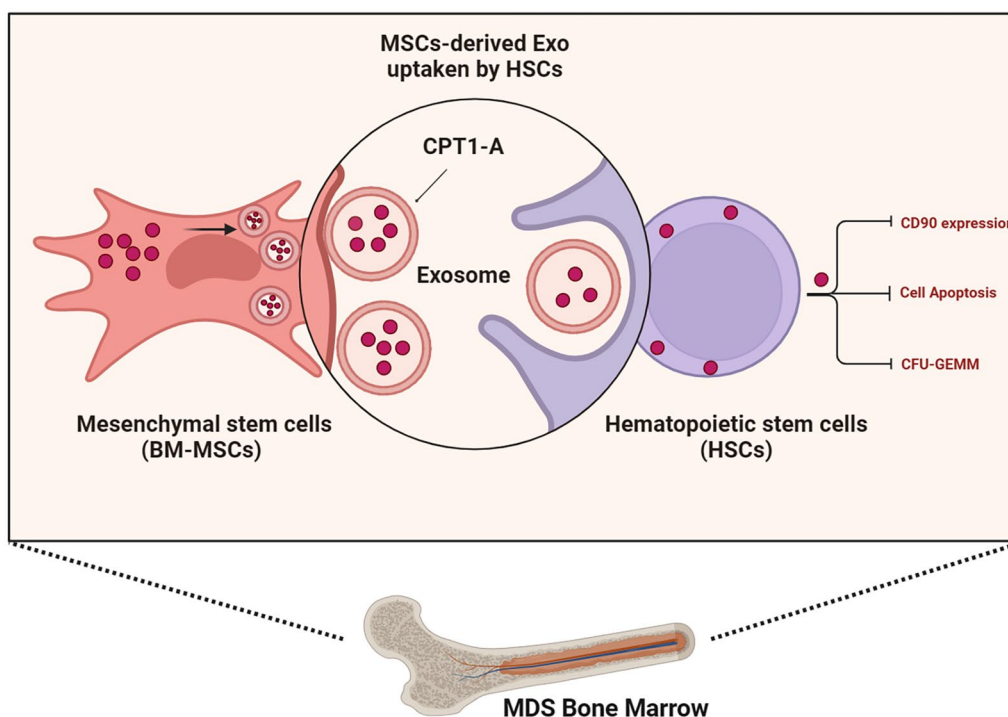


**Fig. 6** Graphical Abstract In summary, our findings suggest that MDS BM microenvironment perturbs MSCs metabolism by enhancing the expression of CPT-1A, which impairs the ability of MSCs to support normal HSCs. Enforcing MSCs lipo-metabolic balance with ETO rescues the suppressed normal hematopoiesis in vitro MDS models. Intriguingly, the suppressive effect is reversible and mediated by exosomes derived from MSCs. These findings shed light on the novel MDS MSCs-metabolism-Exo axis in ineffective hematopoiesis and provide new insights and strategies for the treatment of MDS

exosomes derived from MSCs promote acute myeloid leukemia cell proliferation, invasion and chemoresistance via upregulation of S100A4 [53]. This suggests that exosomes from MSCs or HSCs could serve as mediators of functional transfer between these cell types [2, 54, 55], and will lose their original function in pathological state. We observed that exosomes derived from MDS-BM-MSCs enriched with CPT-1A could inhibit HSCs hematopoiesis. Remarkably, inhibiting the activity of CPT-1A with ETO in MDS-MSCs restored the supportive role of exosomes in HSCs hematopoiesis but not the number. This suggested that the heightened lipid metabolism in supporting cells leads to increased secretion of exosomes enriched with CPT-1A, which may exert their function upon uptake by HSCs through endocytosis. However, further verification is needed to ascertain whether these processes directly influence HSCs function, and the mechanism of action of CPT-1A within HSCs warrants further investigation. While our study provided compelling evidence that MDS-MSCs and their derived exosomes inhibited HSCs hematopoiesis, these findings had yet to be verified within the complex microenvironment of the bone marrow (BM) in vivo.

### Conclusions

In conclusion, our results indicated that MDS bone marrow microenvironment alters the metabolism of MSCs by increasing the expression of CPT-1A which in turn hampered the capacity of MSCs to facilitate normal hematopoiesis in HSCs. Remarkably, this inhibitory effect could be propagated via exosomes that were enriched in CPT-1A and secreted by MSCs (Fig. 6). These discoveries illuminated a novel pathway involving MDS-MSCs, metabolic disturbances, and exosomes in the pathophysiology of ineffective hematopoiesis, providing fresh insights and potential therapeutic approaches for the management of MDS.

### Abbreviations

MDS	Myelodysplastic syndrome
HSCs	Hematopoietic stem cells
MSCs	Mesenchymal stem cells
BM	Bone marrow
ETO	Etomoxir
CPT-1A	Carnitine palmitoyltransferase 1A
SCF	Stem cell factor
IDA	Iron deficiency anemia
MNCs	Mononuclear cells
CFU	Colony forming unit

## Supplementary Information

The online version contains supplementary material available at <https://doi.org/10.1186/s13287-025-04154-3>.

Additional file 1.

Additional file 2.

### Acknowledgements

We thank all the members of Department of Immunology in Dalian Medical University for experimental help and the software support provided by <https://www.biorender.com>.

### Author contributions

Chunlai Yin: Conceptualization, Data curation, Formal analysis, Funding acquisition, Project administration, Resources, Supervision, Visualization, Writing—review and editing. Xue Yan: Investigation, Data curation, Methodology, Writing—original draft. Cheng Zhang: Software, Supervision and Validation. Jinyi Ren and Jiaqing Liu: Investigation and Data curation. Zilong Wang: Software and Writing—review and editing. Jing Liu: Methodology and Supervision. Weiping Li: Writing—review and editing, Visualization, Validation, Project administration, Resources. Xia Li: Writing—review and editing, Visualization, Validation, Project administration, Funding acquisition.

### Funding

This study was supported by the Doctoral Start-up Foundation of Liaoning Province [2021-BS-205]; Basic Research Projects of Liaoning Provincial Department of Education [JYTQN2023152]; Youth Talent Cultivation Fund Project of Dalian Medical University; Dalian Medical University Interdisciplinary Research Cooperation Project Team Funding [JCHZ2023010]; Basic Scientific Research Project (Key Project) of the Education Department of Liaoning Province [LJ212410161034]; National Natural Science Foundation of China [82071834, 82271839].

### Availability of data and materials

All materials and data can be available in the Manuscript and Additional file.

### Declarations

#### Ethics approval and consent to participate

This study was approved by the ethics committee of the Second Hospital of Dalian Medical University. (Approval number: 2019-151). The title of ethical approved project: "Explore the function specific cell molecules in the development of acute myeloid leukemia". Date of approval: 2019/12/12. The authors declare that they have not use AI-generated work in this manuscript.

#### Consent for publication

Not applicable.

#### Competing interest

The authors declare that they have no known competing financial interests or personal relationships that could have appeared to influence the work reported in this paper.

#### Author details

<sup>1</sup>Department of Immunology, College of Basic Medical Science, Dalian Medical University, Dalian 116044, Liaoning, China. <sup>2</sup>College of Pharmacy, Dalian Medical University, Dalian 116044, Liaoning, China. <sup>3</sup>Department of Hematology, the Second Hospital of Dalian Medical University, Dalian 116027, Liaoning, China.

Received: 2 December 2024 Accepted: 17 January 2025

Published online: 07 February 2025

### References

- Ganan-Gomez I, Yang H, Ma F, Montalban-Bravo G, Thongon N, Marchica V, et al. Stem cell architecture drives myelodysplastic syndrome

- progression and predicts response to venetoclax-based therapy. *Nat Med.* 2022;28(3):557–67.
- Hayashi Y, Kawabata KC, Tanaka Y, Uehara Y, Mabuchi Y, Murakami K, et al. MDS cells impair osteolineage differentiation of MSCs via extracellular vesicles to suppress normal hematopoiesis. *Cell Rep.* 2022;39(6):110805.
- Tanaka TN, Bejar R. MDS overlap disorders and diagnostic boundaries. *Blood.* 2019;133(10):1086–95.
- Yin C, Li Y, Zhang C, Zang S, Wang Z, Yan X, et al. Sequential gene expression analysis of myelodysplastic syndrome transformation identifies HOXB3 and HOXB7 as the novel targets for mesenchymal cells in disease. *BMC Cancer.* 2024;24(1):111.
- Garcia-Manero G. Myelodysplastic syndromes: 2023 update on diagnosis, risk-stratification, and management. *Am J Hematol.* 2023;98(8):1307–25.
- Kfoury YS, Ji F, Jain E, Mazzola M, Schirolli G, Papazian A, et al. The bone marrow stroma in human myelodysplastic syndrome reveals alterations that regulate disease progression. *Blood Adv.* 2023;7(21):6608–23.
- Mendez-Ferrer S, Michurina TV, Ferraro F, Mazloom AR, MacArthur BD, Lira SA, et al. Mesenchymal and haematopoietic stem cells form a unique bone marrow niche. *Nature.* 2010;466(7308):829–34.
- Sacchetti B, Funari A, Michienzi S, Di Cesare S, Piersanti S, Saggio I, et al. Self-renewing osteoprogenitors in bone marrow sinusoids can organize a hematopoietic microenvironment. *Cell.* 2007;131(2):324–36.
- Parlindungan F, Damanik J, Araminta AP, Soetedjo AV, Hidayat R, Kusumo Wibowo SA, et al. Mesenchymal stem cell transplantation as a potential therapy for refractory lupus nephritis: a systematic review. *Rheumatol Autoimmun.* 2023;3(3):140–8.
- Kastrinaki MC, Pavlaki K, Batsali AK, Kouvidi E, Mavroudi I, Pontikoglou C, et al. Mesenchymal stem cells in immune-mediated bone marrow failure syndromes. *Clin Dev Immunol.* 2013;2013:265608.
- Nandakumar N, Mohan M, Thilakan AT, Sidharthan HK, Ramu J, Sharma D, et al. Bioengineered 3D microfibrillar-matrix modulates osteopontin release from MSCs and facilitates the expansion of hematopoietic stem cells. *Biotechnol Bioeng.* 2022;119(10):2964–78.
- Pinho S, Frenette PS. Haematopoietic stem cell activity and interactions with the niche. *Nat Rev Mol Cell Biol.* 2019;20(5):303–20.
- Zhou BO, Yu H, Yue R, Zhao Z, Rios JJ, Naveiras O, et al. Bone marrow adipocytes promote the regeneration of stem cells and haematopoiesis by secreting SCF. *Nat Cell Biol.* 2017;19(8):891–903.
- Ferrer RA, Wobus M, List C, Wehner R, Schonefeldt C, Brocard B, et al. Mesenchymal stromal cells from patients with myelodysplastic syndrome display distinct functional alterations that are modulated by lenalidomide. *Haematologica.* 2013;98(11):1677–85.
- Geyh S, Oz S, Cadeddu RP, Frobel J, Bruckner B, Kundgen A, et al. Insufficient stromal support in MDS results from molecular and functional deficits of mesenchymal stromal cells. *Leukemia.* 2013;27(9):1841–51.
- Abbas S, Kumar S, Srivastava VM, Therese MM, Nair SC, Abraham A, et al. Heterogeneity of mesenchymal stromal cells in myelodysplastic syndrome-with multilineage dysplasia (MDS-MLD). *Indian J Hematol Blood Transfus.* 2019;35(2):223–32.
- Corradi G, Baldazzi C, Ocadlikova D, Marconi G, Parisi S, Testoni N, et al. Mesenchymal stromal cells from myelodysplastic and acute myeloid leukemia patients display in vitro reduced proliferative potential and similar capacity to support leukemia cell survival. *Stem Cell Res Ther.* 2018;9(1):271.
- Garrigos MM, de Oliveira FA, Nucci MP, Nucci LP, Alves ADH, Dias OFM, et al. How mesenchymal stem cell cotransplantation with hematopoietic stem cells can improve engraftment in animal models. *World J Stem Cells.* 2022;14(8):658–79.
- Kastrinaki MC, Pontikoglou C, Klaus M, Stavroulaki E, Pavlaki K, Papadaki HA. Biologic characteristics of bone marrow mesenchymal stem cells in myelodysplastic syndromes. *Curr Stem Cell Res Ther.* 2011;6(2):122–30.
- Zhao ZG, Xu W, Yu HP, Fang BL, Wu SH, Li F, et al. Functional characteristics of mesenchymal stem cells derived from bone marrow of patients with myelodysplastic syndromes. *Cancer Lett.* 2012;317(2):136–43.
- Zhao Z, Wang Z, Li Q, Li W, You Y, Zou P. The different immunoregulatory functions of mesenchymal stem cells in patients with low-risk or high-risk myelodysplastic syndromes. *PLoS ONE.* 2012;7(9):e45675.
- Pontikoglou CG, Matheakakis A, Papadaki HA. The mesenchymal compartment in myelodysplastic syndrome: its role in the pathogenesis of the disorder and its therapeutic targeting. *Front Oncol.* 2023;13:1102495.

23. Zhang C, Yang F, Cornelia R, Tang W, Swisher S, Kim H. Hypoxia-inducible factor-1 is a positive regulator of Sox9 activity in femoral head osteonecrosis. *Bone*. 2011;48(3):507–13.
24. Wagegg M, Gaber T, Lohanatha FL, Hahne M, Strehl C, Fangradt M, et al. Hypoxia promotes osteogenesis but suppresses adipogenesis of human mesenchymal stromal cells in a hypoxia-inducible factor-1 dependent manner. *PLoS ONE*. 2012;7(9):e46483.
25. Cianci R, Simeoni M, Cianci E, De Marco O, Pisani A, Ferri C, et al. Stem cells in kidney ischemia: from inflammation and fibrosis to renal tissue regeneration. *Int J Mol Sci*. 2023;24(5):4631.
26. Wang R, Hussain A, Guo QQ, Jin XW, Wang MM. Oxygen and iron availability shapes metabolic adaptations of cancer cells. *World J Oncol*. 2024;15(1):28–37.
27. Shi X, Zhang G, Sun H, Bai Y, Liu Y, Zhang W, et al. Effects of over-expression of HIF-1 $\alpha$  in bone marrow-derived mesenchymal stem cells on traumatic brain injury. *Eng Life Sci*. 2018;18(6):401–7.
28. Noronha NC, Mizukami A, Caliarí-Oliveira C, Cominal JG, Rocha JLM, Covas DT, et al. Priming approaches to improve the efficacy of mesenchymal stromal cell-based therapies. *Stem Cell Res Ther*. 2019;10(1):131.
29. Medyouf H, Mossner M, Jann JC, Nolte F, Raffel S, Herrmann C, et al. Myelodysplastic cells in patients reprogram mesenchymal stromal cells to establish a transplantable stem cell niche disease unit. *Cell Stem Cell*. 2014;14(6):824–37.
30. Sarhan D, Wang J, Sunil Arvindam U, Hallstrom C, Verneris MR, Grzywacz B, et al. Mesenchymal stromal cells shape the MDS microenvironment by inducing suppressive monocytes that dampen NK cell function. *JCI Insight*. 2020. <https://doi.org/10.1172/jci.insight.130155>.
31. Chen W, Yu Y, Zheng SG, Lin J. Human gingival tissue-derived mesenchymal stem cells inhibit proliferation and invasion of rheumatoid fibroblast-like synoviocytes via the CD39/CD73 signaling pathway. *Rheumatol Autoimmun*. 2023;3(2):90–9.
32. Singh AK, Prasad P, Cancelas JA. Mesenchymal stromal cells, metabolism, and mitochondrial transfer in bone marrow normal and malignant hematopoiesis. *Front Cell Dev Biol*. 2023;11:1325291.
33. Arya SB, Collie SP, Parent CA. The ins-and-outs of exosome biogenesis, secretion, and internalization. *Trends Cell Biol*. 2024;34(2):90–108.
34. Zeidan AM, Shallis RM, Wang R, Davidoff A, Ma X. Epidemiology of myelodysplastic syndromes: why characterizing the beast is a prerequisite to taming it. *Blood Rev*. 2019;34:1–15.
35. Stoddart A, Wang J, Hu C, Fernald AA, Davis EM, Cheng JX, et al. Inhibition of WNT signaling in the bone marrow niche prevents the development of MDS in the Apc(del/+) MDS mouse model. *Blood*. 2017;129(22):2959–70.
36. Fujii S, Miura Y, Fujishiro A, Shindo T, Shimazu Y, Hirai H, et al. Graft-versus-host disease amelioration by human bone marrow mesenchymal stromal/stem cell-derived extracellular vesicles is associated with peripheral preservation of naive T cell populations. *Stem Cells*. 2018;36(3):434–45.
37. Budgude P, Kale V, Vaidya A. Cryopreservation of mesenchymal stromal cell-derived extracellular vesicles using trehalose maintains their ability to expand hematopoietic stem cells in vitro. *Cryobiology*. 2021;98:152–63.
38. Finelli C, Parisi S, Paolini S. Exploring the rationale for red cell transfusion in myelodysplastic syndrome patients: emerging data and future insights. *Expert Rev Hematol*. 2022;15(5):411–21.
39. Palacios-Berraquero ML, Alfonso-Pierola A. Current therapy of the patients with MDS: walking towards personalized therapy. *J Clin Med*. 2021;10(10):2107.
40. Alessandrino EP, Della Porta MG, Bacigalupo A, Van Lint MT, Falda M, Onida F, et al. WHO classification and WPSS predict posttransplantation outcome in patients with myelodysplastic syndrome: a study from the Gruppo Italiano Trapianto di Midollo Osseo (GITMO). *Blood*. 2008;112(3):895–902.
41. Shi Y, Du L, Lin L, Wang Y. Tumour-associated mesenchymal stem/stromal cells: emerging therapeutic targets. *Nat Rev Drug Discov*. 2017;16(1):35–52.
42. Christopher AC, Venkatesan V, Karuppusamy KV, Srinivasan S, Babu P, Azhagiri MKK, et al. Preferential expansion of human CD34(+)CD133(+)CD90(+) hematopoietic stem cells enhances gene-modified cell frequency for gene therapy. *Hum Gene Ther*. 2022;33(3–4):188–201.
43. Karuppusamy KV, Demosthenes JP, Venkatesan V, Christopher AC, Babu P, Azhagiri MKK, et al. The CCR5 gene edited CD34(+)CD90(+) hematopoietic stem cell population serves as an optimal graft source for HIV gene therapy. *Front Immunol*. 2022;13:792684.
44. Jajosky AN, Coad JE, Vos JA, Martin KH, Senft JR, Wenger SL, et al. RepSox slows decay of CD34+ acute myeloid leukemia cells and decreases T cell immunoglobulin mucin-3 expression. *Stem Cells Transl Med*. 2014;3(7):836–48.
45. Zhai Y, Meng F, Li J, Ma J, Shen L, Zhang W. Upregulation of S100A6 and its relation with CD34(+) cells apoptosis in high-risk myelodysplastic syndromes patients. *Heliyon*. 2023;9(8):e18947.
46. Bayley R, Blakemore D, Cancian L, Dumon S, Volpe G, Ward C, et al. MYBL2 supports DNA double strand break repair in hematopoietic stem cells. *Cancer Res*. 2018;78(20):5767–79.
47. Carter BZ, Mak PY, Muftuoglu M, Tao W, Ke B, Pei J, et al. Epichaperome inhibition targets TP53-mutant AML and AML stem/progenitor cells. *Blood*. 2023;142(12):1056–70.
48. Du W, Xu A, Huang Y, Cao J, Zhu H, Yang B, et al. The role of autophagy in targeted therapy for acute myeloid leukemia. *Autophagy*. 2021;17(10):2665–79.
49. Li X, Wang X, Zhang C, Wang J, Wang S, Hu L. Dysfunction of metabolic activity of bone marrow mesenchymal stem cells in aged mice. *Cell Prolif*. 2022;55(3):e13191.
50. Pouikli A, Tessarz P. Metabolism and chromatin: a dynamic duo that regulates development and ageing: elucidating the metabolism-chromatin axis in bone-marrow mesenchymal stem cell fate decisions. *BioEssays*. 2021;43(5):e2000273.
51. Li H, Dai H, Li J. Immunomodulatory properties of mesenchymal stromal/stem cells: the link with metabolism. *J Adv Res*. 2023;45:15–29.
52. Chen Q, Yuan Y, Chen T. Morphology, differentiation and adhesion molecule expression changes of bone marrow mesenchymal stem cells from acute myeloid leukemia patients. *Mol Med Rep*. 2014;9(1):293–8.
53. Lyu T, Wang Y, Li D, Yang H, Qin B, Zhang W, et al. Exosomes from BM-MSCs promote acute myeloid leukemia cell proliferation, invasion and chemoresistance via upregulation of S100A4. *Exp Hematol Oncol*. 2021;10(1):24.
54. Muntion S, Ramos TL, Diez-Campelo M, Roson B, Sanchez-Abarca LI, Misiewicz-Krzeminska I, et al. Microvesicles from mesenchymal stromal cells are involved in HPC-microenvironment crosstalk in myelodysplastic patients. *PLoS ONE*. 2016;11(2):e0146722.
55. Yin C, Han Q, Xu D, Zheng B, Zhao X, Zhang J. SALL4-mediated upregulation of exosomal miR-146a-5p drives T-cell exhaustion by M2 tumor-associated macrophages in HCC. *Oncoimmunology*. 2019;8(7):1601479.

## Publisher's Note

Springer Nature remains neutral with regard to jurisdictional claims in published maps and institutional affiliations.